Nanotechnology, Science and Applications

Dovepress
Taylor & Francis Group

Open Access Full Text Article

ORIGINAL RESEARCH

Silver Nanoparticles Attenuate Histamine-Induced Pruritus via Modulation of the Nitric Oxide/iNOS Signaling Pathway in Mice

Abdul Mobin Bayan[1], Muhammad Imran Khan[2]

[1]Department of Pharmaceutical Chemistry, Faculty of Pharmacy, Maihan University, Kabul, Afghanistan; [2]Department of Biological and Health Sciences, Pak-Austria Fachhochschule, Institute of Applied Sciences and Technology, Haripur, Pakistan

Correspondence: Abdul Mobin Bayan; Muhammad Imran Khan, Email Mobin.bayan@Maihan.edu.af; imran.khan@fbse.paf-iast.edu.pk

Background: Pruritus is an unpleasant cutaneous sensation that provokes scratching behavior and is associated with numerous inflammatory and dermatological disorders. Histamine is a major mediator of pruritus and contributes to the activation of inflammatory and oxidative stress pathways. Silver nanoparticles (Ag-NPs) possess well-documented anti-inflammatory, antioxidant, antimicrobial, and wound-healing properties. The present study investigated the antipruritic effects of Ag-NPs and the involvement of the nitric oxide (NO) signaling pathway in histamine-induced pruritus in mice.

Methods: Silver nanoparticles were synthesized using a green synthesis approach and characterized by UV–Vis spectroscopy, FTIR, and SEM analyses. Histamine-induced pruritus was established in male NMRI mice by intradermal injection of histamine (400 µg) into the shaved nape of the neck. Ag-NPs were administered intraperitoneally at doses of 1, 1.5, and 2 mg/kg. To investigate the role of nitric oxide signaling, mice received the nitric oxide synthase inhibitors Nω-Nitro-L-arginine methyl ester (L-NAME, 1 mg/kg) or aminoguanidine (AG, 200 mg/kg) prior to histamine administration. Scratching behavior was recorded, while oxidative stress markers, nitric oxide levels, nerve growth factor (NGF), inducible nitric oxide synthase (iNOS) expression, and histopathological changes were evaluated.

Results: Histamine administration increased scratching behavior, nitric oxide production, nerve growth factor (NGF) levels, oxidative stress, and iNOS gene expression in mouse skin tissue. Treatment with Ag-NPs significantly reduced histamine-induced scratching and attenuated nitric oxide production. Ag-NPs also improved antioxidant status by increasing glutathione, glutathione S-transferase, and catalase levels while reducing lipid peroxidation. Furthermore, Ag-NPs treatment significantly decreased NGF levels and suppressed iNOS mRNA expression. Histopathological examination revealed marked improvement in skin architecture and reduced tissue damage in Ag-NP-treated groups. The antipruritic effects of Ag-NPs were further enhanced in combination with nitric oxide synthase inhibitors, suggesting the involvement of the NO/iNOS signaling pathway.

Conclusion: Silver nanoparticles exhibit antipruritic activity against histamine-induced pruritus in mice. Their protective effects are associated with suppression of the NO/iNOS pathway, reduction of oxidative stress, modulation of NGF expression, and attenuation of inflammatory responses. These findings suggest that Ag-NPs may represent a promising therapeutic strategy for the management of pruritic disorders.

Keywords: pruritus, silver nanoparticles, histamine, neural growth factors, inducible nitric oxide synthase, mice, oxidative stress

Introduction

Pruritus is an unpleasant cutaneous sensation that elicits an urge to scratch and is commonly associated with a variety of dermatological and systemic disorders. Given its persistent and distressing nature, the impact of pruritus-induced stress on both physiological functions and social behaviors should not be underestimated, as it can substantially impair an individual's quality of life and overall well-being.[1] Owing to high prevalence, pruritus is among the 50 most common diseases worldwide. Developing countries experience a significant burden, with approximately 70% of their population affected, often accompanied by other related skin disorders. Pruritus can significantly diminish a person's life quality, leading to sleep disturbances, anxiety, depression, and disruption the daily quality of life.[2]

https://doi.org/10.2147/NSA.S591039
Received: 21 January 2026
Accepted: 18 June 2026
Published: 3 July 2026

The severity and duration of pruritus depend on the underlying cause and individual characteristics such as age, sex, and skin type. The duration of pruritus is divided into two main categories: acute and chronic pruritus. Acute pruritus is short-term pruritus that typically lasts for a few hours or days. Acute itching is associated with insect bites, allergic reactions, and dermatitis. Once the underlying cause is addressed, itching subsides. Histamine is a biogenic amine stored in the secretory granules of mast cells and basophils that normally contributes to anaphylaxis and allergy. It is released during immunological reactions the skin.[3]

Histamine is released in response to various stimuli such as allergens, physical stimuli, and emotional stress. Histamine causes itching when it is produced and binds to receptors on the sensory nerve fibers. Histamine increases the activity of nitric oxide synthase, an enzyme responsible for the producing of oxide.[4] Histamine exerts its effects by binding to specific histamine receptors on the target cells. Activation of the H2 receptor by histamine can increase intracellular calcium levels, triggering calcium release from intracellular stores localized in the endoplasmic reticulum, which regulates many cellular processes, including the activity of NOS isoforms.[5] The increase in intracellular calcium levels caused by histamine stimulation can lead to the formation of a calcium-calmodulin complex. The calcium-calmodulin complex acts as a second messenger and plays a crucial role in activating NOS, which is triggered by a conformational change in the enzyme that activates its catalytic activity domain. This activation allows NOS to convert l-arginine into nitric oxide (NO) and citrulline. Nitric oxide is a signaling molecule involved in physiological functions, such as the regulation of blood flow, neurotransmission, and immune response.[6]

Ag-NPs are a group of zero-dimensional nanoparticles with specific shapes and dimensions ranging from 1 to 100 nm, and each particle has approximately 15 tail and 1000 silver (Ag) atoms.[7] Previous studies have demonstrated that Ag-NPs suppress the production of pro-inflammatory cytokines, inhibit inducible nitric oxide synthase (iNOS) activity, reduce oxidative stress, and promote tissue repair. The viability of these nanoparticles has been demonstrated in the design and development of improved wound healing. Human skin has various semi-open pores into which silver ions can penetrate, mostly in the form of silver protein complexes.[8] To reduce the harmful effects of silver, green synthesis is emerging as a new field in which biological materials such as plant extracts or microorganisms are used for the synthesis of silver nanoparticles as an alternative to chemical methods, which is highly biological and environmentally friendly.[9] *Melilotus indicus* was selected as the reducing and stabilizing agent for the green synthesis of Ag-NPs because it is rich in bioactive phytochemicals, including phenolic compounds, flavonoids, coumarins, and other antioxidant constituents. These phytochemicals can facilitate the reduction of silver ions to metallic silver while simultaneously acting as capping agents that enhance nanoparticle stability.

The reaction between silver nanoparticles (Ag-NPs) and enzymes can inhibit enzyme activity through mechanisms such as binding to the active site. Ag-NPs can interact directly with the active site of an enzyme, which is the region where the other substrate normally binds and is catalyzed. By occupying the active site, Ag-NPs prevent the substrate from accessing the enzyme and inhibit the catalytic reaction. Nerve Growth Factor (NGF) is a crucial protein that is essential for the development and maintenance of nerve cells. Produced by neurons, immune cells, and skin cells during inflammation, nerve growth factors are influenced by pro-inflammatory cytokines.[10] Therefore, the present study was designed to investigate the antipruritic effects of green-synthesized silver nanoparticles (Ag-NPs) in a histamine-induced murine model of pruritus. In addition, the study aimed to elucidate the involvement of nitric oxide signaling, particularly inducible nitric oxide synthase (iNOS), as well as oxidative stress and nerve growth factor (NGF)-related pathways, in mediating the antipruritic activity of Ag-NPs.

Materials and Methods

Chemical & Reagents

Silver nanoparticles (Ag-NPs) were synthesized according to the previously reported method.[11] Histamine was purchased from Shanxi Pharma (Shanghai, China). Histamine was obtained from Shanxi Pharma (Shanghai, China). Glutathione (GSH), Nω-nitro-L-arginine methyl ester (L-NAME), 1-chloro-2,4-dinitrobenzene (CDNB), hydrogen peroxide (H_2O_2), 5,5′-dithiobis-(2-nitrobenzoic acid) (DTNB), aminoguanidine (AG), and thiobarbituric acid reactive substances (TBARS) assay reagents were purchased from Sigma-Aldrich (St. Louis, MO, USA).

The mouse nerve growth factor (NGF) ELISA kit (Catalog No. PRS-30462Ra) was purchased from Nanjing PARS Biochem Co., Ltd. (Nanjing, China). Primers for inducible nitric oxide synthase (iNOS) gene expression analysis were obtained from Afnan Traders (Pakistan).

All other analytical-grade chemicals and reagents, including Griess reagent, phosphate-buffered saline (PBS), TRIzol reagent, normal saline, absolute ethanol, xylene, hematoxylin, and eosin, were supplied by the Department of Biomedical Sciences, PAF Institute of Applied Sciences and Technology (PAF-IAST), Pakistan.

Silver Nanoparticle's Synthesis

Silver nanoparticles (Ag-NPs) were synthesized using the aqueous leaf extract of *Melilotus indicus* as a green reducing and stabilizing agent. Fresh, healthy leaves of *M. indicus* were collected from Hangu, Pakistan. Briefly, 10 g of freshly collected leaves were washed thoroughly, boiled in 100 mL of distilled water for 7 min, and subsequently homogenized using a laboratory grinder. The resulting extract was filtered through Whatman No. 1 filter paper to remove particulate matter.

For nanoparticle synthesis, a 3 mM aqueous silver nitrate ($AgNO_3$) solution was prepared in a 250 mL beaker containing 100 mL of distilled water. The reaction vessel was sealed with Parafilm to minimize solvent evaporation and stirred magnetically at 40 °C for 1 h. Thereafter, 15 mL of the prepared plant extract was added dropwise to the silver nitrate solution, and the reaction mixture was continuously stirred at room temperature for 3 h. The phytoconstituents present in the extract acted as reducing, capping, and stabilizing agents, facilitating the conversion of silver ions into Ag-NPs.

The reaction mixture was subsequently transferred to a Teflon-lined autoclave and subjected to hydrothermal treatment at 150 °C for 12 h. Following synthesis, the nanoparticles were collected by centrifugation at 3500 rpm for 10 min, washed several times with deionized water to remove residual impurities, and dried at 80 °C for 5 h. The dried Ag-NPs were then stored for further physicochemical characterization and biological evaluation.[11]

Characterization of Ag-NPs

The formation of Ag-NPs was investigated using UV-vis spectroscopy in the range 200–700 nm wavelength. Scanning electron microscopy (SEM; JSM-IT100, JEOL, Japan) was employed to analyze the surface morphology, size, and structural characteristics of the synthesized silver nanoparticles (Ag-NPs). For sample preparation, small quantity of the dried Ag-NP powder was dispersed in distilled water and sonicated to obtain a uniform suspension. A drop of this suspension was carefully placed onto a clean aluminum stub covered with carbon tape and allowed to air-dry at room temperature. To enhance conductivity and image resolution, the samples were subsequently sputter-coated with a thin layer of gold prior to SEM analysis.[12] FTIR spectra were used to determine the functional groups available in nanoparticles an ABB-MB3000 spectrophotometer, and the data were analyzed using Origin and ImageJ software.

Ethical Approval and Animal Handling

Adult male NMRI mice weighing 24–30 g were obtained from the National Institute of Health (NIH), Islamabad, Pakistan. The animals were acclimatized to the laboratory environment for one week prior to the initiation of the experiments. Mice were randomly assigned to seven experimental groups, with five animals in each group. Throughout the study period, the animals were housed under standardized environmental conditions, including a controlled temperature of 25 ± 2 °C, relative humidity of 50–60%, and a 12 h light/12 h dark cycle. Standard laboratory chow and water were provided ad libitum. Bedding material was replaced every three days to maintain hygiene and minimize the risk of environmental allergens that could influence pruritic responses. All experimental procedures were conducted in accordance with institutional guidelines for the care and use of laboratory animals. Ethical approval for the study was obtained from the Pak-Austria Institutional Research Ethics Committee (Approval No. PAF-IAST/2023/10).

The study followed the principles outlined in the guide for the care and use of laboratory animals and the American Veterinary Medical Association (AVMA) Guidelines for the Euthanasia. At the end of the behavioral observation period mice were anesthetized using an intraperitoneal injection of ketamine (80–100 mg/kg) and xylazine (10–12.5 mg/kg) to achieve deep surgical anesthesia confirmed by the absence of reflex responses. Following anesthesia were performed in accordance with AVMA recommendations ensuring rapid loss of consciousness and minimization of pain and distress.

Death was verified by the absence of respiratory effort and cardiac activity prior to tissue collection, in line with AVMA guidelines.

Pharmacological Experiments

In the control group, normal saline was administered intraperitoneally at a dose of 10 mL/Kg body weight and the skin of the mice was collected from the shaved part of the neck for further study.[13] For pruritus induction histamine were administrated at dose of 400 µg intradermally at the nap of the neck where the heir previously removed. The silver nanoparticle suspension was administered intraperitoneally at doses of (1, 1.5, and 2 mg/kg),[14] separately and in combination with histamine. To study the role of NO synthase in this experimental group, a suspension of Ag-NPs was administered intraperitoneally at a dosage of 1.5 mg/kg body weight. Thirty minutes after the nanoparticle injection, L-NAME (200 mg/kg) was administered at a dosage of 1 mg/kg aminoguanidine.[15] After 30 min, the histamine was injected. Moreover a 0.25 mL/kg dose of cetirizine was administered IP as a positive control. The experimental protocol was conducted over a period of 14 days.

Behavior Studies

Histamine Induced Pruritus Model

In the histamine-induced scratching model, mice were first acclimatized under controlled laboratory conditions at 25 °C. Following histamine administration to induce pruritic behavior, the animals were individually placed in a transparent glass observation chamber designed for behavioral assessment. Scratching behavior was then recorded under undisturbed conditions, with no observer present in the immediate environment, to minimize external influence and ensure unbiased behavioral evaluation.[16] The video was reviewed to document the frequency of hind paw scratching at the site of injection, defining a single scratch as any contact made with the shaved area, and a scratching movement within a one-second frame was considered as one bout of scratching. Activities involving the front limbs were excluded from scratch counts. The observation period was an hour and samples were collected for further analysis.

Molecular Study

Antioxidant Assay

Skin samples were homogenized in PBS and centrifuged at 4000 rpm for 30 min to remove debris. The resulting supernatant was used to measure the levels of four oxidative stress markers. Glutathione (GSH) levels were determined by measuring the oxidation of GSH, 5,5′-dithiobis (2-nitrobenzoic acid) (DTNB) conjugate, and sodium phosphate buffer to produce a yellow product. The absorbance of this product was measured at 412 nm using a microplate reader, and GSH values were expressed as micromoles per milligram of protein. Glutathione S-transferase (GST) levels were assessed by measuring the formation of the 1-chloro-2,4-dinitrobenzene (CDNB) conjugate, with absorbance at 340 nm using a microplate reader. Catalase activity was measured by monitoring hydrogen peroxide (H2O2) degradation using a 340 nm microplate reader, with moles of H2O2 degraded per minute and milligrams of degraded protein. The lipid peroxidase-LPO level was measured using an absorbance 532 nm microplate reader, the collected supernatant was mixed with TBARS + potassium phosphate buffer and stored in a water bath at 37 °C for 1 h after centrifugation at 2500 (for 10 min). The LPO content was expressed in the microplate reader in nmol per minute per milligram of protein.[17]

Measurement of Nitrite in Histamine Induced Pruritus Skin Sample

A series of sodium nitrite reference solutions was prepared using PBS to construct an accurate calibration curve essential for nitric oxide measurement. Subsequently, an equal volume of 50 µL of the tissue extract and 50 µL of sterile saline solution was amalgamated with a corresponding quantity of the Griess reagent, The reactants were by incubation for 30 min at temperature of 37°C. This incubation period facilitates the conversion of nitrites in the specimen to a chromogenic azo dye upon reaction with the Griess reagent. The absorbance of the resulting solution was determined at a wavelength of 546 nm using an ELISA microplate reader and compared to the absorbance values of standard sodium nitrite solutions.[18]

Enzyme-Linked Immunosorbent Assay (ELISA) for Neural Growth Factor (NGF) Level Determination

ELISA for mouse skin neural growth factor (NGF) was conducted according to the manufacturer's instructions. An appropriate quantity already stored in freezer −80 °C, of skin tissues (50 mg) sample homogenized in PBS (50 mg of skin sample in 0.5 mL the supernatant was collected after centrifuging the homogenate sample at (4000 rpm for 30 min) from insoluble debris. Sandwich ELISA immunosorbent assay was used to determine the total NGF protein concentration in each group. NGF samples were treated with the antibodies provided in the kit in a 96-well plate. 14 wells coated with 100 µL, of standard and 50 µL standard dilution, the blank wells separately considered as testing wells for supernatant in duplicate, 40 µL sample dilution were added in the wells, the testing sample were added 10 µL in every well the plat closed by closure plate membrane and incubated for 30 minutes in 37°C after that wash solution diluted 20-fold with distilled water, the plat uncovered the liquid discarded and washing buffer added in each well, after washing the 50 µL HRP conjugate regent were added in each well except blanks, the incubation and washing treated again respectively. In the next step, 50 µL of chromogen solutions A and B was added to each well and the light was preserved for 15 min, after which 50 µL of stop, solution was added to each well to stop the reaction. After 15 minutes the absorbance explored at 450 nm microplate reader used to evaluate the absorbance, values and concentrations were converted to picograms per milligram of total protein (pg/mg total protein), which served as the new standard.[19]

Revers Transcription Polymerase Chain Reaction (RT-PCR) for Inducible Nitric Oxide Synthase Expression in Pruritus Model Skin Sample

The RNA extracted from stored tissue samples at −80°C using TRIzol method.[20] RNA quality was determined using a Nanodrop to check purity. Forward and reverse primers were designed for iNOS using (Primer 3 blast, Figure 1) and (UCSC in silico) software, and alignment sequence (Clustal omega w) software was used. For complementary DNA synthesis the RT reaction was prepared by mixing 1 µg of RNA template with 70 ng/µL oligo primers and RNase-free water to adjust the total reaction volume, which was then incubated 65 °C for 5 min to denature the RNA and then cooled on ice. The denatured sample was mixed gently with 2 µL RT buffer, 2 µL dNTPs, and 1 µL RT enzyme and incubated 42 °C for 50 min to synthesize cDNA. For amplification of iNOS and the reference gene GAPDH the cDNA template was mixed with the designed primers, PCR reaction buffer, and RNase free water. PCR amplification was performed using a thermal cycler under appropriate cycling conditions for both iNOS and the reference genes. iNOS and reference gene expression were determined by CFX-96 Bio-Rad (RT-PCR), and the values were calculated according to the cycle threshold (CT) and fold expression of target genes.

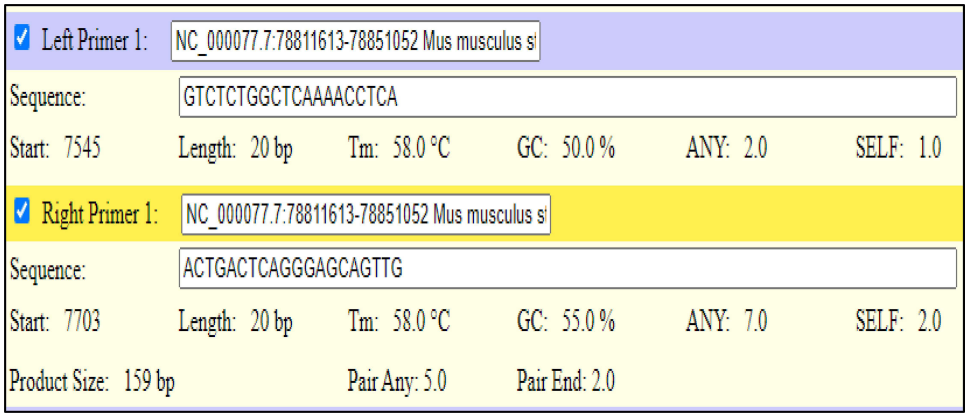

Figure 1 Designed forward and revers primers for inducible nitric oxide synthase (iNOS) gene.

https://doi.org/10.2147/NSA.S591039

Histological Analysis

The stored sample in 10% formalin at 4°C were assigned to a distinct cassette for processing. The HISTI-PRO-300 processor used a 10% paraformaldehyde solution as the initial fixative.[21] The samples were then dehydrated through several concentrations of 50% increasing to 75% and finally 95% ethanol. Following dehydration, xylene was used as a clarifying agent, and each skin sample was immersed for one hour. The tissues were then fused with molten paraffin wax in a three-cycle process to ensure thorough embedding, and then stored in a cooling module to solidify the wax. After solidification, the tissue blocks were cut into 5 µm sections using an automated microtome. These sections were floated in deionized water and carefully aligned onto glass slides. For Staining, tissue-bearing slides were submerged in xylene for 35 min. A sequential rehydration process was performed in descending concentrations of ethanol for 35 min. The slides were then stained using a 3-minute submersion in hematoxylin to color the nuclei blue and then rinsed in tap water to wash away the excess stain. Eosin was then applied for one minute to impart a red or pink color to the cytoplasm and to other extracellular components. The slides were dehydrated using an ascending ethanol series and cleared in xylene. Finally, a drop of DPX mounting medium was applied to each slide and the slide was sealed with a coverslip. High resolution images at 10x magnification were captured using a light microscope.

Statistical Analyses

The data are expressed as the mean ± standard error of the mean. GraphPad Prism version 10 was used to conduct statistical analyses, which included a one-way analysis of variance followed by Tukey's post hoc test for multiple comparisons.

Findings

Synthesis of Silver Nanoparticles Using UV–Visible Spectroscopy

The synthesis of silver nanoparticles (Ag-NPs) was confirmed using UV–visible spectroscopy. The recorded spectrum exhibited a characteristic absorption band in the range of approximately 300–350 nm, which is consistent with the surface plasmon resonance (SPR) of Ag-NPs. The absorbance intensity was observed to increase from approximately 0.6 to 1.0, indicating successful nanoparticle formation and enhanced optical activity. These findings support the presence of well-formed Ag-NPs with relatively uniform characteristics, further suggesting their suitability for subsequent biological and physicochemical applications.

Fourier Transform Infrared Spectroscopy (FTIR) Analysis

FTIR was used to investigate the interactions between the functional groups present in green-synthesized Ag-NPs. The observed peaks in the FTIR spectra highlight the involvement of organic components responsible for both the reduction and stabilization of Ag-NPs. Different peaks were observed at 3324 cm^{-1}, indicating the presence of O-H bonds, while the peak at 2094 cm^{-1} was attributed to CH_2 stretching the appearance of a peak at 1632 cm^{-1} suggested the involvement of a carbonyl moiety, and the fingerprinting region revealed a prominent peak at 424 cm^{-1}, which validated the successful synthesis of Ag-NPs (Figure 2).

Scanning Electron Microscope Analysis

Scanning electron microscopy (SEM) was performed to investigate the structural and morphological characteristics of the green-synthesized silver nanoparticles (Ag-NPs). The SEM micrographs at different magnifications (Figure 3) demonstrated that the nanoparticles were predominantly well distributed, with a generally uniform morphology. Particle size analysis performed using ImageJ software revealed an average particle size in the range of 8–20 nm, based on initial estimations from SEM images. Although most nanoparticles appeared discrete, some degree of agglomeration was observed, which may be attributed to interparticle interactions and the inherent tendency of nanoparticles to cluster during synthesis and drying processes. Overall, the observed morphological features are consistent with previously reported studies on biologically synthesized Ag-NPs.

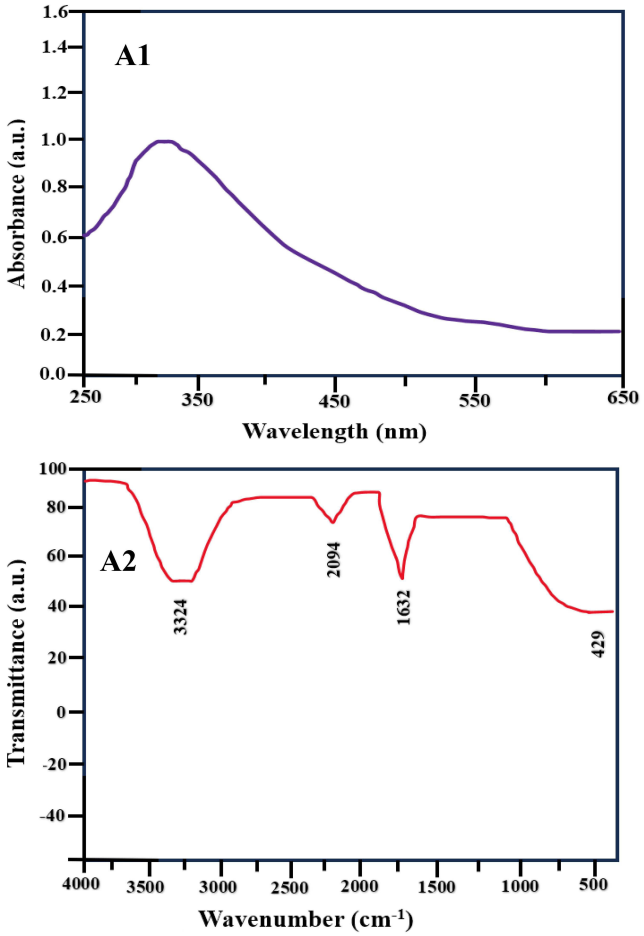

Figure 2 (A1) Comparative UV-Vis Spectroscopy and (**A2**) FTIR Analysis of Silver Nanoparticles.

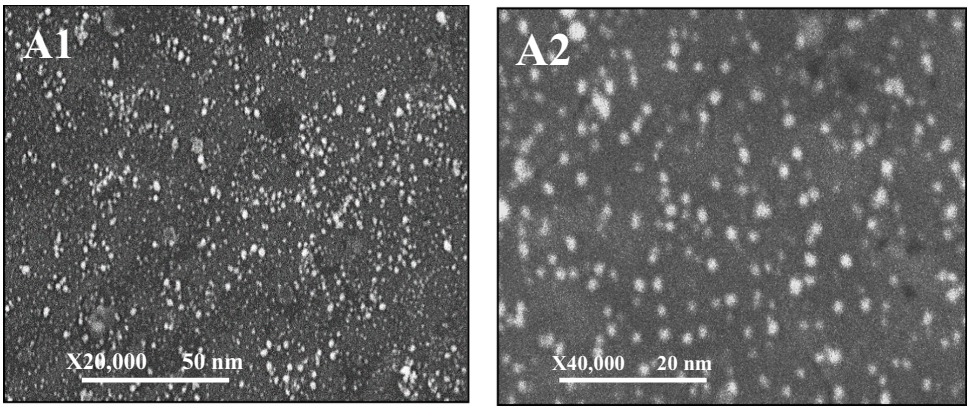

Figure 3 (**A1**) and (**A2**) SEM images in different magnification and size distribution of silver nanoparticles.

Behavior Result

Effect of Silver Nanoparticles Against Histamine-Induced Pruritus Behavioral Analysis

Histamine, a potent mediator known to stimulate itch via histaminergic receptors, was used to validate the experimental pruritus model. During our controlled study, mice administered histamine displayed a significantly increased frequency of scratching behaviors indicating pruritus compared to the control group treated with saline (Figure 4, $^{###}P < 0.001$). Notably, the administration of silver nanoparticles concomitantly with histamine significantly reduced scratching behavior ***P <

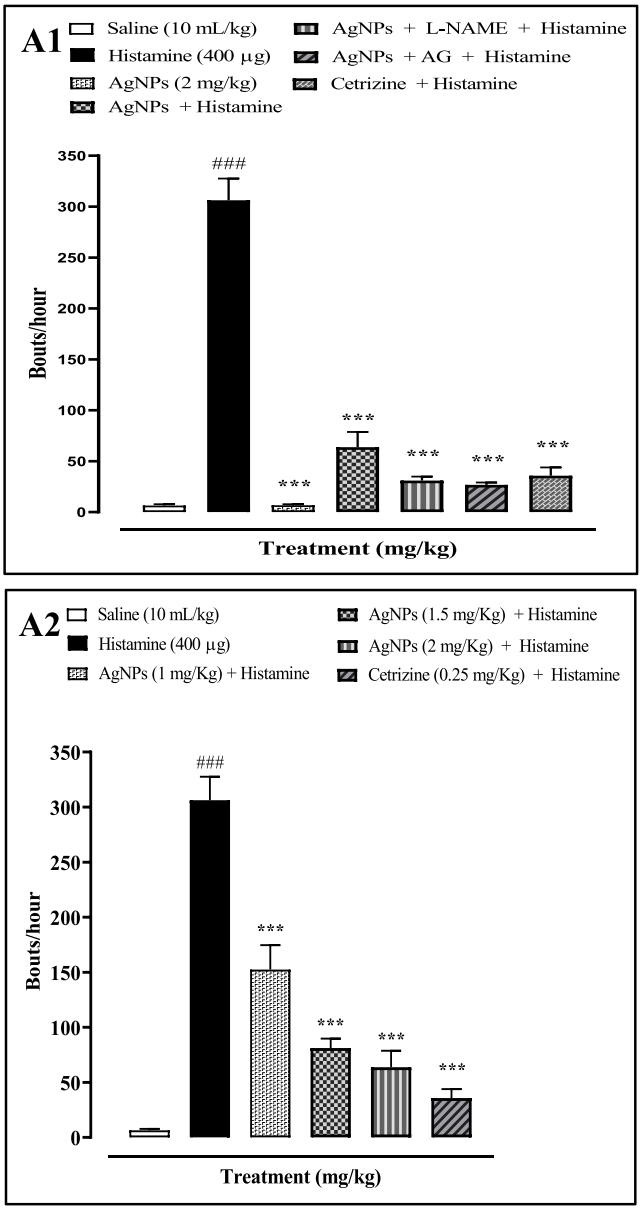

Figure 4 Graph (**A1**) shows the hourly scratching frequency in mice receiving various treatments, including saline, histamine, silver nanoparticles (Ag-NPs), Ag-NPs combined with L-NAME or AG, and cetirizine in combination with histamine. Data represent the mean ± SEM (n = 3) per group. Statistical analysis was performed using one-way ANOVA followed by Tukey's post hoc test. ###P < 0.001 versus the saline group; ***P < 0.001 versus the histamine-treated group. Graph (**A2**) shows the effects of different doses of Ag-NPs (1, 1.5, and 2 mg/kg) on histamine-induced scratching of mouse skin tissue. ###P < 0.001 versus the saline group; ***P < 0.001 versus the histamine-treated group.

0.001, suggesting an antagonistic effect of the nanoparticles on histaminergic induced pruritus, potentially through the modulation of receptor interactions or downstream signaling cascades. In behavioral analyses the histamine group exhibited an average of 300 scratching bouts per hour, whereas the groups treated with Ag-NPs displayed a substantial decrease in such behaviors. Interestingly, the group treated solely with Ag-NPs did not exhibit a significant difference from the saline group, underscoring the specificity of the pruritus-mitigating effect of nanoparticles.

The involvement of the nitric oxide pathway in pruritus was further investigated by administering AG, which is known to suppress inducible nitric oxide synthase, and L-NAME, an inhibitor of NOS which consequently reduces nitric oxide synthesis. The variations in behavioral responses across each group emphasized the impact of experimental factors on the observed pruritus in mice.

Additionally, this study included cetirizine, an antihistamine that blocks histamine H1 receptors, to evaluate its pruritic effect in comparison with Ag-NPs. The results demonstrated that Mice treated with Ag-NPs exhibited scratching bouts similar to those treated with cetirizine, emphasizing the potential of Ag-NPs as a comparable inhibitor of histamine-induced pruritus in this animal model.

These data collectively suggest that Ag-NPs can modulate the pruritus response by interfering with the nitric oxide pathway, proposing an alternative therapeutic approach to traditional antihistamines in the management of itch.

Molecular Study

Effect of Silver Nanoparticles on Nitrite Levels on Histamine-Induced Pruritus

To evaluate the effect of silver nanoparticles (Ag-NPs) on nitric oxide (NO) production in histamine-induced pruritus, nitrite levels, an indirect indicator of NO generation, were quantified using the Griess assay. Histamine administration resulted in a significant elevation of nitrite levels compared with the control group, indicating enhanced NO production. In contrast, co-administration of Ag-NPs with histamine markedly reduced nitrite concentrations relative to the histamine-treated group. A comparable reduction in nitrite levels was observed in animals treated with nitric oxide synthase inhibitors and/or cetirizine following histamine induction (Table 1). Overall, treatment with Ag-NPs, nitric oxide synthase inhibitors, and cetirizine significantly modulated NO production, suggesting the involvement of the nitric oxide signaling pathway in the antipruritic effects observed in this study.

Effect of Silver Nanoparticles on Oxidative Stress Markers

The antioxidant potential of silver nanoparticles (Ag-NPs) was evaluated in skin tissues obtained from mice subjected to histamine-induced pruritus. Oxidative stress was assessed by measuring four key biomarkers, including lipid peroxidation (LPO), glutathione (GSH), glutathione S-transferase (GST), and catalase activity. Histamine administration resulted in a significant increase in LPO levels (###$P < 0.001$) compared with the control group, indicating enhanced oxidative damage. Concurrently, significant reductions in GSH content, GST activity, and catalase activity were observed, reflecting impaired antioxidant defense mechanisms (Figure 5).

Treatment with Ag-NPs significantly attenuated histamine-induced oxidative stress, as evidenced by decreased LPO levels and restoration of GSH, GST, and catalase activities. Similar protective effects were observed when Ag-NPs were administered in combination with nitric oxide synthase inhibitors, including L-NAME and aminoguanidine (AG). These findings suggest that Ag-NPs exert a protective effect against histamine-induced oxidative damage by enhancing endogenous antioxidant defenses, thereby contributing to the alleviation of pruritic responses and the maintenance of skin tissue integrity (Figure 5).

Effect of Silver Nanoparticles on Neural Growth Factor in Mouse Skin Sample

A quantitative enzyme-linked immunosorbent assay (ELISA) was conducted to measure nerve growth factor (NGF) levels in mouse skin tissues subjected to histamine-induced pruritus. The results showed an increase in NGF

Table 1 This Table Represents the Effect of Ag-NPs, N-Nitro-L-Arginine Methyl Ester (L-NAME), Aminoguanidine (AG) and Cetirizine on the Formation of Nitric Oxide (NO) in Histamine-Induced Pruritus in Mice Skin Tissues Using Nitrate Measurement

Treatment Group	Nitric Oxide (µmol/mg Protein)
Normal Saline (10 mL/kg)	42.45 ± 2.2
Histamine (400 µg)	134.23 ± 2###
Ag-NPs (2 mg/kg) + Histamine (400 µg)	102.32 ± 1.33*
Ag-NPs (1.5 mg/kg) + L-NAME (1 mg/kg) + Histamin (400 µg)	95.55 ± 1.22**
Ag-NPs (1.5 mg/kg) + AG (200 mg/kg) + Histamine (400 µg)	85.12 ± 2***
Cetirizine (0.25 mg/kg) + Histamine (400 µg)	72.41 ± 1.64***

Notes: Data are presented as mean ± SEM for triplicates (n=3). Statistical significance was determined using one-way ANOVA followed by Tukey's post-hoc test, with ###$P < 0.001$ vs. saline group, and *$P < 0.05$, **$P < 0.01$, ***$P < 0.001$ vs. histamine group.

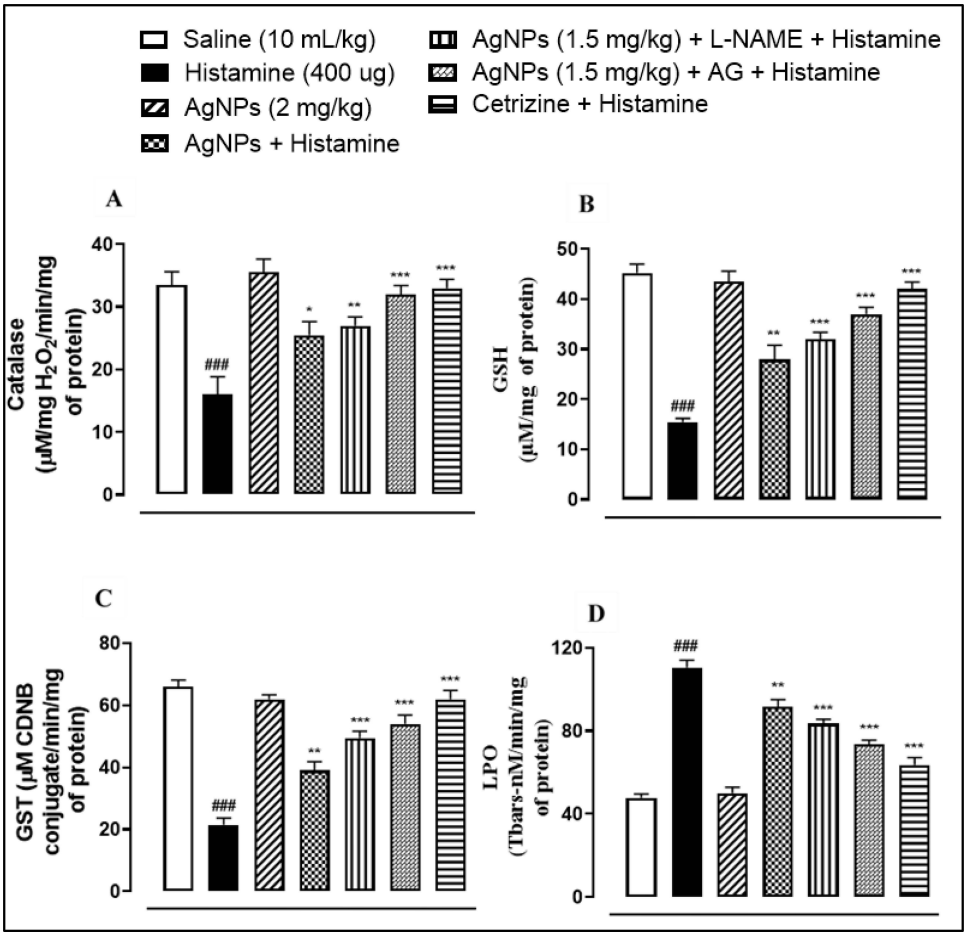

Figure 5 Effect of Ag-NPs, inhibiters and cetirizine against in combination to histamine on (**A**) Catalase, (**B**) decreased glutamine (GSH), (**C**) glutathione s-transferase (GST) and (**D**) increased lipid peroxidase (LPO) in Histamine-induced pruritus in mice skin tissue. Values analyzed as mean ± SEM (n=5). One way ANOVA with post hoc Tukey's test. ###P < 0.001 vs. saline group, only Ag-NPs has no significance vs saline group, *P < 0.05, **P < 0.01, ***P < 0.001 vs. Histamine group.

concentration in the histamine-treated group compared to the saline control group ($P < 0.001$), underscoring the pro-inflammatory role of NGF in the histamine-mediated inflammatory response. In contrast, treatment with silver nanoparticles (Ag-NPs) did not lead to a statistically significant change in NGF levels compared to the saline control, suggesting that Ag-NPs have a neutral effect on NGF expression in this model. The groups treated with (L-NAME) and aminoguanidine showed a pronounced decrease in NGF levels ($P < 0.001$) suggesting a mitigating effect on histamine-induced NGF overexpression. The group treated with cetirizine, an established antihistamine, also showed a significant decrease in NGF levels ($P < 0.01$), further validating the anti-inflammatory potential of cetirizine in histamine-induced pruritus. These findings collectively imply that the tested inhibitors, particularly L-NAME and AG, are potent modulators of NGF expression, possibly through interaction with the NO pathway, and may thus represent a viable therapeutic strategy against inflammatory pruritus, Figure 6.

Effect of Silver Nanoparticles on Expression of iNOS Level in Mouse Skin Sample

Modulation of iNOS expression by Ag-NPs was evaluated in mouse skin samples. The evaluation utilized the RT-PCR was performed to quantify iNOS transcriptional levels. Comparative analysis revealed that in the histamine administered disease group, there was a 2.7-fold increase in the transcription of iNOS mRNA when compared with the unaltered expression observed in the control group. Conversely, treatment regimens comprising Silver Nanoparticles, the general inhibitor L-NAME, the specific inhibitor, and a combination of cetirizine and histamine significantly attenuated iNOS mRNA transcription levels relative to the histamine-only treated group as shown in Figure 7. These observations show the potential of Ag-NPs and implicated nitric oxide pathway mediators in mitigating the upregulation of iNOS associated with pruritic responses.

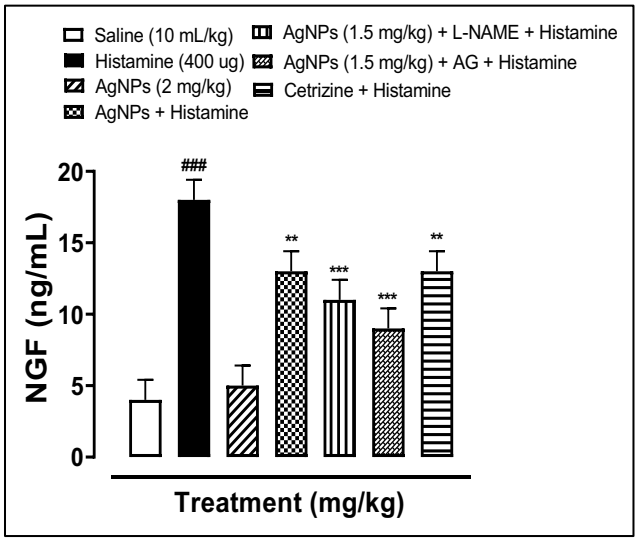

Figure 6 Comparative Analysis of Nerve Growth Factor (NGF) Modulation in Mouse Skin Samples Following Induction of Pruritus by Histamine: Data are presented as mean ± SEM for n=5 per group. Statistical significance determined by one-way ANOVA followed by Tukey's post hoc analysis: ### indicates P < 0.001 compared to the saline-treated control; **P < 0.01, and ***P < 0.001 indicate statistical significance compared to the Histamine-only treated group. The Ag-NPs treatment alone showed no statistically significant difference from the Saline control.

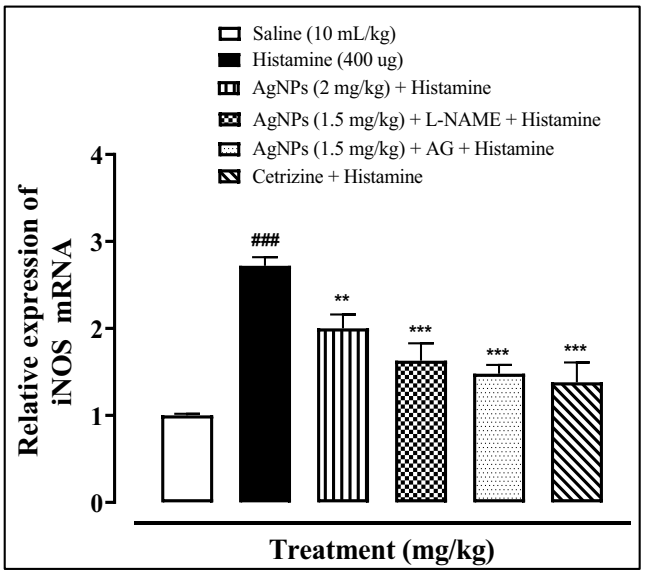

Figure 7 Revealed modulation of iNOS mRNA levels in the skin tissue of mice with histamine-induced pruritus, as assessed by RT-PCR. The graph quantifies the mean SEM, (n=3). Statistical significance was determined by one-way ANOVA and subsequent Tukey's post hoc test: ### indicates ***P < 0.001 when compared to the saline-treated reference group, **P < 0.01 and ***P < 0.001, respectively, against the histamine-treated benchmark.

Histopathological Evaluation of Therapeutic Interventions on Histamine-Induced Dermal Tissue Alterations in Mice

Histological assessment of the skin tissue in a pruritic mouse model highlighted the profound impact of histamine on skin integrity. The saline (10 mL/kg) group showed a normal skin tissue appearance without any pathological changes. The histamine treated group displayed significant morphological disruptions, including epidermal damage with increased thickness, extensive tissue necrosis, and compromised membrane integrity across both epidermal and dermal layers. In contrast, therapeutic interventions with silver nanoparticles (Ag-NPs), alone or in combination with nitric oxide synthase inhibitors such as L-NAME and AG, as well as the antihistamine cetirizine, demonstrated notable reversal of the deleterious effects induced by histamine. The treated groups showed markedly less morphological damage, reduced cell necrosis, and an overall improvement in tissue architecture. These treatments notably improved the integrity and normalization of the epidermal layer, showing restorative effects as reflected in the data illustrated in Figure 8.

https://doi.org/10.2147/NSA.S591039

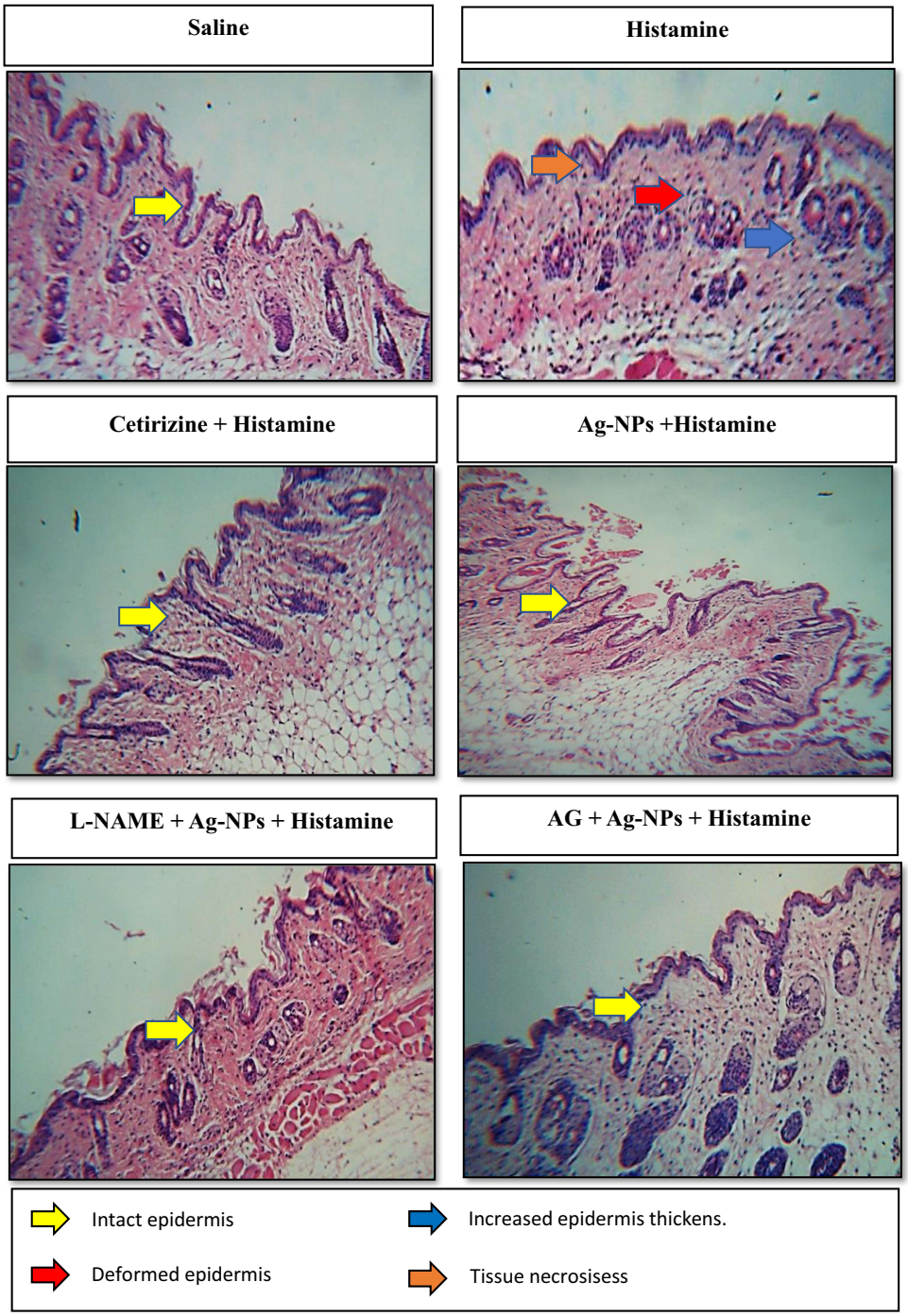

Figure 8 Shows the assessment of histopathological alterations in mouse dermal tissue following histamine-induced scratching: a histological comparison using Hematoxylin and Eosin (H&E) staining.

Discussion

Histamine is a well-established mediator of pruritus and exerts its effects primarily through the activation of H1 and H4 receptors expressed on cutaneous sensory nerve fibers. Binding of histamine to these receptors initiates a complex cascade of intracellular signaling events that activate itch-specific neuronal pathways, ultimately resulting in the perception of itching and the induction of scratching behavior. Previous studies have demonstrated that H1 receptor activation is primarily responsible for acute histaminergic itch, whereas H4 receptor signaling contributes to immune cell recruitment and the amplification of inflammatory responses associated with chronic pruritic conditions. Consistent with

these findings, histamine administration in the present study induced a robust pruritic response, supporting the suitability of the histamine-induced mouse model for investigating antipruritic interventions. These observations are in agreement with earlier reports highlighting the central role of histamine-mediated signaling in the pathogenesis of allergic and inflammatory skin disorders.[22] The binding of histamine to these receptors triggers a cascade of neuronal signaling that culminates in the perception of itching, a characteristic symptom of various allergic and inflammatory skin conditions.[23] Therapeutically, the efficacy of antihistamines in mitigating itching demonstrates integral role of histamine in pruritic pathways. Ongoing research continues to unravel the complexities of histamine action in pruritus, paving the way for more targeted and effective treatment. The search for effective therapies in modern medicine often focuses on symptom management rather than tackling the root causes of diseases, leading to treatments that may be too harsh for use as preventive measures. Historically, natural compounds have been at the forefront of medicinal practice, offering holistic remedies for various ailments and injuries. In contemporary biomedical research, silver nanoparticles (Ag-NPs) have emerged as a sign of hope primarily because of their broad-spectrum antimicrobial properties. These nanoparticles, synthesized using bioactive compounds derived from natural sources, not only serve as reducing and stabilizing agents but also exhibit pronounced anti-inflammatory properties. The "green" synthesis of Ag-NPs is particularly notable, as it ensures efficacy with safety, demonstrating a potent inhibitory effect on a variety of pathogens, including bacteria, fungi, and viruses, with minimal associated toxicity.[24] These nanoparticles are hypothesized to facilitate wound repair by promoting cellular activities essential for regeneration, such as keratinocyte proliferation, migratory enhancement, and increased collagen synthesis.[25] Moreover, various studies have demonstrated the versatile therapeutic potential of Ag-NPs, ranging from enhanced wound healing to protection against UV-induced skin damage. As exploration into nanoparticle technology continues, it is imperative to consider both the therapeutic efficacy and safety profile of these nanomaterials to ensure their beneficial application in dermatological treatments.[26] As shown in fig.3.4, Ag-NPs significantly inhibited the histamine-induced scratching effect ($p<0.001$). Our study is in line with other studies, which found that oral administration of ZnO-NPs significantly reduced chloroquine-induced pruritus in a murine model.[27]

Nitric oxide is a gaseous, short-lived, and unstable signaling molecule found in various dermatological and neuropsychiatric disorders. The current findings also demonstrate that the NO pathway is involved in the antipruritic effects of Ag-NPs. When the sub-effective dose of Ag-NPs was co-treated with a sub-effective dose of NOS inhibitors, the histamine-induced scratching behavior was significantly alleviated, as shown in fig. 3.3. and fig.3.4. In the brain nitric oxide synthase is catalyzed by NOS isoforms from l-arginine.[4] Nitric oxide (NO) plays a significant role in skin inflammation. In pruritic conditions like atopic eczema and psoriasis it is observed by researchers that overproduction of nitric oxide contributes to those conditions.[28] The interaction between histamine and cutaneous cells of the skin when contracting allergens significantly enhances the production of pro-inflammatory cytokines, nerve growth factor (NGF), and markers indicative of oxidative stress, suggesting potent inflammatory cascade activation within the skin.[29] In response, intraperitoneal administration of nitric oxide synthase inhibitors, such as N-nitro-L-arginine methyl ester (L-NAME) and aminoguanidine (AG), has been investigated to determine the involvement of nitric oxide. Notably, a specific dosage of silver nanoparticles (Ag-NPs) of 1 mg/kg, in combination with an AG inhibitor, has shown efficacy in diminishing histamine-induced cutaneous nitric oxide (NO) levels, hinting at a targeted inhibitory effect on the intradermal NO pathway. iNOS catalyzes the production of nitric oxide (NO) in response to pro-inflammatory stimuli and has various functions in the body, including immune response regulation, neurotransmission[30.] Nitric oxide can react with other molecules to form reactive nitrogen species, which can damage cellular structures and foreign molecules.[30] In our study we further demonstrated through RT-PCR that iNOS is iNOS in the induction of pruritus. The iNOS mRNA levels were significantly higher in the histamine group than in the control group. In the silver nanoparticle ($p<0.01$), L-NAME-($p<0.001$), AG($p<0.001$), and cetirizine ($p<0.001$) treated groups, the expression level of iNOS mRNA was significantly decreased compared to that in the disease group. Hence, our study confirms the potential involvement of iNOS in histamine-induced pruritus.

In the search for novel anti-pruritic agents, silver nanoparticles (Ag-NPs) have demonstrated significant promising effects owing to their intrinsic antioxidant properties and their ability to scavenge free radicals. The efficacy of Ag-NPs has been substantiated through biochemical assays of lipid peroxidation (LPO), catalase activity, glutathione S-transferase (GST), and reduced glutathione (GSH), indicating that Ag-NPs modulate oxidative stress parameters in the skin.[31] Notably the role of histamine in exacerbating oxidative stress is evident by its ability to elevate LPO while

diminishing the concentrations of GST, GSH, catalase, enzymes, and substrates critical in the body's defense against oxidative damage.[32] Conversely, the application of Ag-NPs, both independently and synergistically with nitric oxide synthase inhibitors such as L-NAME and AG, was associated with a ($P < 0.05$), ($P < 0.01$), and ($P < 0.001$) reversal of these effects. The observed upregulation of GSH, GST, and catalase, along with the reduced levels of LPO in the treated models, supports the hypothesis that antioxidants can attenuate the sensation of itch by reducing oxidative stress.[33]

The interaction between the immune system and neural functions is complicated and leads to upregulation of nerve growth factor (NGF) during inflammatory states. The increase in NGF expression is vital in the body's defense, not only in terms of modulation of immune responses but also in ensuring the maintenance and survival of neuronal cells under stress. In the present study, Ag-NPs exerted modulatory effects on NGF expression. The results of ELISA demonstrated quantitative evidence, where it was significantly increased in histamine induced pruritus compared to the control group. However, Ag-NPs significantly reduced NGF overexpression. Specifically, Ag-NPs appear to downregulate the heightened levels of NGF, which are typically induced by pro-inflammatory agents such as histamine. Similarly, interventions with Ag-NPs and cetirizine significantly decreased these elevations. This attenuation of NGF by Ag-NPs could be essential for developing therapeutic strategies aimed at controlling neurogenic inflammation, providing a molecular basis for their anti-inflammatory potential.[34] Using different experimental and molecular approaches, it was confirmed that Ag-NPs have an anti-scratching effect mediated through oxidative stress/NGF/NO pathways. Future studies may explore the potential synergistic effects of laser-assisted silver nanoparticle therapy, as photonic stimulation has been reported to enhance the biological and therapeutic activities of nanoparticles in various biomedical applications.

Conclusion

The present study was designed to investigate the antipruritic effects of silver nanoparticles (Ag-NPs) and to explore the involvement of nitric oxide-related signaling pathways in histamine-induced pruritus in mice. The findings demonstrated that Ag-NPs reduced histamine-induced scratching behavior and improved histopathological alterations in skin tissue. Furthermore, Ag-NPs attenuated oxidative stress by decreasing lipid peroxidation and enhancing antioxidant defense mechanisms, while also suppressing the overexpression of nerve growth factor (NGF) and inducible nitric oxide synthase (iNOS). The enhanced antipruritic effects observed following co-administration of nitric oxide synthase inhibitors further support the involvement of the NO/iNOS signaling pathway in the mechanism of action of Ag-NPs. Collectively, these findings suggest that silver nanoparticles exert antipruritic activity through modulation of oxidative stress, NGF, and NO/iNOS pathways and may represent a promising therapeutic approach for the management of pruritic disorders. Further studies are warranted to evaluate their long-term safety and clinical applicability.

Data Sharing Statement

The data supporting the findings of this study are available from the corresponding author upon reasonable request.

Acknowledgments

We extend our appreciation to Dr. Muhammad Imran Khan for his valuable supervision, insightful guidance, and continuous support throughout this research. His expertise and constructive feedback greatly contributed to the successful completion of this study.

Author Contributions

All authors made a significant contribution to the work reported, whether that is in the conception, study design, execution, acquisition of data, analysis and interpretation, or in all these areas; took part in drafting, revising or critically reviewing the article; gave final approval of the version to be published; have agreed on the journal to which the article has been submitted; and agree to be accountable for all aspects of the work.

Funding

This research received no specific grants from any funding agency or from commercial or non-profit sectors.

Disclosure

The authors declare that they have no known competing financial interests, personal relationships, or any other conflict of interest that could have influenced the work reported in this study.

References

1. Agarwal P, Garg V, Karagaiah P, Szepietowski JC, Grabbe S, Goldust M. Chronic kidney disease-associated pruritus. *Toxins*. 2021;13(8):527. doi:10.3390/toxins13080527
2. Kahremany S, Hofmann L, Harari M, Gruzman A, Cohen G. Pruritus in psoriasis and atopic dermatitis: current treatments and new perspectives. *Pharmacol Rep*. 2021;73(2):443–453. doi:10.1007/s43440-020-00206-y
3. Kabashima K, Nakashima C, Nonomura Y, et al. Biomarkers for evaluation of mast cell and basophil activation. *Immunol Rev*. 2018;282 (1):114–120. doi:10.1111/imr.12639
4. Haddadi NS, Shakiba S, Afshari K, et al. Possible involvement of nitric oxide in the antipruritic effect of metformin on chloroquine-induced scratching in mice. *Dermatology*. 2020;236(2):151–159. doi:10.1159/000501583
5. Beretta M, Santos CX, Molenaar C, et al. Nox4 regulates InsP3 receptor-dependent Ca2+ release into mitochondria to promote cell survival. *EMBO J*. 2020;39(19):e103530. doi:10.15252/embj.2019103530
6. Wu G, Meininger CJ, McNeal CJ, Bazer FW, Rhoads JM. Role of L-arginine in nitric oxide synthesis and health in humans. In: *Amino Acids in Nutrition and Health*. Springer; 2021:167–187.
7. Lakkim V, Reddy MC, Pallavali RR, et al. Green synthesis of silver nanoparticles and evaluation of their antibacterial activity against multidrug-resistant bacteria and wound healing efficacy using a murine model. *Antibiotics*. 2020;9(12):902. doi:10.3390/antibiotics9120902
8. Xu L, Wang YY, Huang J, Chen CY, Wang ZX, Xie H. Silver nanoparticles: synthesis, medical applications and biosafety. *Theranostics*. 2020;10 (20):8996. doi:10.7150/thno.45413
9. Parmar S, Kaur H, Singh J, Matharu AS, Ramakrishna S, Bechelany M. Recent advances in green synthesis of Ag NPs for extenuating antimicrobial resistance. *Nanomaterials*. 2022;12(7):1115. doi:10.3390/nano12071115
10. Peirce JM, Alviña K. The role of inflammation and the gut microbiome in depression and anxiety. *J Neuroscienn Res*. 2019;97(10):1223–1241. doi:10.1002/jnr.24476
11. Bukhary HA, Zaman U, Ur Rehman K, et al. Acid protease functionalized novel silver nanoparticles (APTs-Ag-NPs): a new approach towards photocatalytic and biological applications. *Int J Biol Macromol*. 2023;242:124809. doi:10.1016/j.ijbiomac.2023.124809
12. Mouzaki M, Maroui I, Mir Y, et al. Green synthesis of silver nanoparticles and their antibacterial activities. *Green Processing Synth*. 2022;11 (1):1136–1147. doi:10.1515/gps-2022-0061
13. Wan X, Eguchi A, Fujita Y, et al. Effects of (R)-ketamine on reduced bone mineral density in ovariectomized mice: a role of gut microbiota. *Neuropharmacology*. 2022;213:109139. doi:10.1016/j.neuropharm.2022.109139
14. Sousa A, Azevedo R, Costa VM, et al. Biodistribution and intestinal inflammatory response following voluntary oral intake of silver nanoparticles by C57BL/6J mice. *Arch Toxicol*. 2023;97(10):2643–2657. doi:10.1007/s00204-023-03558-5
15. Rahimi N, Modabberi S, Faghir-Ghanesefat H, et al. The possible role of nitric oxide signaling and NMDA receptors in allopurinol effect on maximal electroshock-and pentylenetetrazol-induced seizures in mice. *Neurosci lett*. 2022;778:136620. doi:10.1016/j.neulet.2022.136620
16. Xu RQ, Ma L, Chen T, Zhang WX, Chang K, Wang J. Sophorolipid inhibits histamine-induced itch by decreasing PLC/IP3R signaling pathway activation and modulating TRPV1 activity. *Sci Rep*. 2023;13(1):7957. doi:10.1038/s41598-023-35158-9
17. Yang Y, Pan Y, Liu B, et al. Neutrophil-derived oxidative stress contributes to skin inflammation and scratching in a mouse model of allergic contact dermatitis via triggering pro-inflammatory cytokine and pruritogen production in skin. *Biochem Pharmacol*. 2024;223:116163. doi:10.1016/j.bcp.2024.116163
18. Seemab K, Khan A, Khan MI, Qazi NG, Minhas AM, Ali F. Anti-pruritic effect of L-carnitine against chloroquine-induced pruritus mediated via nitric oxide pathway. *BMC Pharmacol Toxicol*. 2024;25(1):32. doi:10.1186/s40360-024-00748-4
19. Want A, Morgan JE, Barde YA. Brain-derived neurotrophic factor measurements in mouse serum and plasma using a sensitive and specific enzyme-linked immunosorbent assay. *Sci Rep*. 2023;13(1):7740. doi:10.1038/s41598-023-34262-0
20. Kumar K, Oli A, Hallikeri K, Shilpasree AS, Goni M. An optimized protocol for total RNA isolation from archived formalin-fixed paraffin-embedded tissues to identify the long non-coding RNA in oral squamous cell carcinomas. *MethodsX*. 2022;9:101602. doi:10.1016/j.mex.2021.101602
21. Khatoon H, Sahana NS, Suresh T, Tahasildar J, Renuga S, Kulkarni M. Effect of duration of fixation with formalin on mRNA expression using quantitative RT-PCR. *J Oral Maxillofacial Pathol*. 2025;29(2):186–192. doi:10.4103/jomfp.jomfp_178_24
22. Fukasawa T, Yoshizaki-Ogawa A, Enomoto A, Miyagawa K, Sato S, Yoshizaki A. Pharmacotherapy of itch—antihistamines and histamine receptors as G protein-coupled receptors. *Int J Mol Sci*. 2022;23(12):6579. doi:10.3390/ijms23126579
23. Alatawi RA, Bukhari AAH, Al-Sayed HM, et al. Production of biologically active non-woven textiles from recycled polyethylene terephthalate. *Luminescence*. 2023;38(3):350–359. doi:10.1002/bio.4462
24. Paladini F, Pollini M. Antimicrobial silver nanoparticles for wound healing application: progress and future trends. *Materials*. 2019;12(16):2540. doi:10.3390/ma12162540
25. Rudrappa M, Kumar RS, Nagaraja SK, et al. Myco-nanofabrication of silver nanoparticles by Penicillium brasilianum NP5 and their antimicrobial, photoprotective and anticancer effect on MDA-MB-231 breast cancer cell line. *Antibiotics*. 2023;12(3):567. doi:10.3390/antibiotics12030567
26. Aman N, Rauf K, Khan SA, Tokhi A, Rehman NU, Yameen MA. Effect of commercial and green synthesized ZnO NPs in murine model of chloroquine-induced pruritus. *Int J Nanomed*. 2019;2019:3103–3110. doi:10.2147/IJN.S202256
27. Kim JH, Choi MS. Nitric oxide signal transduction and its role in skin sensitization. *Biomolecules Ther*. 2023;31(4):388. doi:10.4062/biomolther.2023.101
28. Han M, Lee D, Lee SH, Kim TH. Oxidative stress and antioxidant pathway in allergic rhinitis. *Antioxidants*. 2021;10(8):1266. doi:10.3390/antiox10081266

29. Pinheiro MBM, Rozini SV, Quirino-Teixeira AC, et al. Dengue induces iNOS expression and nitric oxide synthesis in platelets through IL-1R. *Front Immunol*. 2022;13:1029213. doi:10.3389/fimmu.2022.1029213
30. Estes LM, Singha P, Singh S, et al. Characterization of a nitric oxide (NO) donor molecule and cerium oxide nanoparticle (CNP) interactions and their synergistic antimicrobial potential for biomedical applications. *J Colloid Interface Sci*. 2021;586:163–177. doi:10.1016/j.jcis.2020.10.081
31. Gorini F, Tonacci A. Tumor microbial communities and thyroid cancer development—the protective role of antioxidant nutrients: application strategies and future directions. *Antioxidants*. 2023;12(10):1898. doi:10.3390/antiox12101898
32. Younis NS, El Semary NA, Mohamed ME. Silver nanoparticles green synthesis via cyanobacterium Phormidium sp.: characterization, wound healing, antioxidant, antibacterial, and anti-inflammatory activities. *Eur Rev Med Pharmacol Sci*. 2021;25(7):1.
33. El Baassiri MG, Dosh L, Haidar H, et al. Nerve growth factor and burn wound healing: update of molecular interactions with skin cells. *Burns*. 2023;49(5):989–1002. doi:10.1016/j.burns.2022.11.001
34. Chen H, Zhang J, Dai Y, Xu J. Nerve growth factor inhibits TLR3-induced inflammatory cascades in human corneal epithelial cells. *J Inflam*. 2019;16(1):27. doi:10.1186/s12950-019-0232-0